Available online at www.sciencedirect.com
ScienceDirect
ELSEVIER
C. R. Physique 8 (2007) 661–673
COMPTES RENDUS
PHYSIQUE
http://france.elsevier.com/direct/COMREN/

Work, dissipation, and fluctuations in nonequilibrium physics

Nonequilibrium decay of the thermal diffusion in a tilted periodic potential

Takaaki Monnai [a,*], Ayumu Sugita [b], Katsuhiro Nakamura [b]

[a] *Department of Applied Physics, Waseda University, 3-4-1 Okubo, Shinjuku-ku, Tokyo 169-8555, Japan*
[b] *Department of Applied Physics, Osaka City University, 3-3-138 Sugimoto, Sumiyoshi-ku, Osaka 558-8585, Japan*

Received 25 April 2007

Available online 28 June 2007

Abstract

We investigate asymptotic decay phenomena towards the nonequilibrium steady state of the thermal diffusion in a periodic potential in the presence of a constant external force. The parameter dependence of the decay rate is revealed by investigating the Fokker–Planck (FP) equation in the low temperature case under the spatially periodic boundary condition (PBC). We apply the WKB method to the associated Schrödinger equation. While eigenvalues of the non-Hermitian FP operator are complex in general, in a small tilting case accompanied with local minima, the imaginary parts of the eigenvalues are almost vanishing. Then the Schrödinger equation is solved with PBC. The decay rate is analyzed in the context of quantum tunneling through a triple-well effective periodic potential. In a large tilting case, the imaginary parts of the eigenvalues of the FP operator are crucial. We apply the complex-valued WKB method to the Schrödinger equation with the absorbing boundary condition, finding that the decay rate saturates and depends only on the temperature, the period of the potential and the damping coefficient. The intermediate tilting case is also explored. The analytic results well agree with the numerical data for a wide range of tilting. Finally, in the case that the potential includes a higher Fourier component, we report the slow relaxation, which is taken as the resonance tunneling. In this case, we analytically obtain the Kramers type decay rate. ***To cite this article: T. Monnai et al., C. R. Physique 8 (2007).***

Résumé

Décroissance de non-équilibre de la diffusion thermique dans un potentiel périodique incliné. Nous examinons le phénomène de décroissance asymptotique vers l'état stationnaire de non-équilibre pour la diffusion thermique dans un potentiel périodique incliné en présence d'une force externe constante. La dépendance paramétrique du taux de décroissance est mise en évidence en examinant l'équation de Fokker–Planck (FP) dans le cas de basse température sous des conditions aux bords périodiques spatiallement (CBP). Nous appliquons la méthode WKB à l'équation de Schrödinger associée. Alors que les valeurs propres de l'opérateur de FP non-hermitien sont en général complexes, les parties imaginaires des valeurs propres sont presque nulles dans le cas d'une petite inclinaison accompagnée par des minima locaux. L'équation de Schrödinger est alors résolue avec les CBP. Le taux de décroissance est analysé dans le contexte de l'effet tunnel quantique à travers un potentiel périodique effectif avec trois puits. Dans le cas d'une grande inclinaison, les parties imaginaires des valeurs propres de l'opérateur de FP sont cruciales. Nous appliquons la méthode WKB sur les complexes à l'équation de Schrödinger avec des conditions aux bords absorbants. Nous trouvons que le taux de décroissance sature et dépend seulement de la température, de la période du potentiel et du coefficient

* Corresponding author.
E-mail addresses: monnai@suou.waseda.jp (T. Monnai), sugita@a-phys.eng.osaka-cu.ac.jp (A. Sugita), nakamura@a-phys.eng.osaka-cu.ac.jp (K. Nakamura).

1631-0705/$ – see front matter
doi:10.1016/j.crhy.2007.05.013

d'amortissement, respectivement. Le cas d'une inclinaison intermédiaire est aussi exploré. Les résultats analytiques sont en bon accord avec les données numériques sur un large domaine d'inclinaison. Finalement, dans le cas où le potentiel inclut une composante de Fourier d'ordre supérieur, nous mettons en évidence une relaxation lente qui est comprise comme un phénomène de résonance d'effet tunnel. Dans ce cas, nous obtenons analytiquement le taux de décroissance du type de Kramers. ***Pour citer cet article : T. Monnai et al., C. R. Physique 8 (2007).***

Keywords: Decay rate; Thermal diffusion; Tilted periodic potential; WKB analysis; Fokker–Planck equation; Resonance tunneling

Mots-clés : Taux de décroissance ; Diffusion thermique ; Potentiel périodique incliné ; Analyse WKB ; Équation de Fokker–Planck ; Résonance d'effet tunnel

1. Introduction

A thermal diffusion process in a periodic potential in the presence of external force often appears in solid-state physics, such as diffusion of ions or molecules on crystal surfaces [1], in Josephson junctions [2] and also in biophysical ratchet systems [3,4]. In particular, it gives a reasonable model of the molecular motors [5]. Most research in this context is concerned with the nonequilibrium steady state. For example, a symmetric dichotomous noise is pointed out to cause non-zero steady state current in such a system [6], and the analytic expression of the diffusion coefficient is reported with emphasis on the existence of its optimal value against an external force [7].

On the other hand, since the monumental work by van Kampen [8], the relaxation process of bistable potential has received considerable attention [9,10], because, within the WKB approximation, we can evaluate the decay rate analytically. In the context of protein crystallization [11], Nicolis and his coworkers [12] reported the enhancement of the decay rate due to the existence of the intermediate state with the aid of the so-called Kramers theory. Recently the role of an intermediate state for crystallization as well as the extension of the Kramers rate to the double-humped barrier are explored with the aid of WKB method [13]. For Langevin systems with colored noise, under the weak damping assumption, the corresponding Fokker–Planck equation is derived and the structure of staggered ladder-spectra is revealed [14].

All of these studies on decay processes, however, are concerned with the relaxation towards the equilibrium state. It is thus of interest to investigate the relaxation towards a nonequilibrium steady state (NESS). In fact, as discussed in the next section, the decay to NESS demands a qualitatively different treatment from the relaxation to equilibrium.

Noting these circumstances, we take a first step to extending the existing theory and investigate the simplest model of the relaxation towards NESS, i.e. the decay in a tilted periodic potential. Such decay processes have practical importance in the context of the ratchet-induced transport theory, because the probability current under natural boundary condition loses its initial form typically within the inverse of the decay rate. As the periodic potential we first choose a simple sinusoidal potential and then a more general one including a higher Fourier component.

Consider a diffusion process in a tilted periodic potential, described by the over-damped Langevin equation

$$\eta\dot{x}(t) = -\frac{\partial}{\partial x}U^{(0)}(x) + \frac{2\pi W}{L}x + \xi(t)$$
$$\langle\xi(t)\rangle = 0, \quad \langle\xi(t)\xi(t')\rangle = 2\eta\theta\delta(t-t') \tag{1}$$

Here, η, $\theta = k_B T$ and W are the damping coefficient, temperature and the external force, respectively. $\xi(t)$ is the Langevin force which satisfies the fluctuation dissipation theorem. The periodic potential $U^{(0)}(x+L) = U^{(0)}(x)$ with period L is tilted by the external tilting force $F = \frac{2\pi W}{L}$, and we call the potential $U(x) \equiv U^{(0)}(x) - \frac{2\pi W}{L}x$ a tilted potential.

In order to investigate the probability density $P(x,t)$ that the particle is found in a position x at a time t, it is useful to transform the Langevin equation into the corresponding Fokker–Planck (FP) equation,

$$\frac{\partial}{\partial t}P(x,t) = \frac{1}{\eta}\frac{\partial}{\partial x}\left(\frac{\partial U(x)}{\partial x} + \theta\frac{\partial}{\partial x}\right)P(x,t) \tag{2}$$

Hereafter we solve the FP equation (2) under the (spatially) periodic boundary condition (PBC), $P(x+L,t)=P(x,t)$, which is satisfied by the steady state at $t\to\infty$. The analytic expression for the steady state $P^{\rm st}(x)\equiv\lim_{t\to\infty}P(x,t)$ under PBC is well-known [5,16,17]:

$$P^{\rm st}(x)=N\frac{\eta}{\theta}\mathrm{e}^{-\frac{U(x)}{\theta}}\int_x^{x+L}\mathrm{d}y\,\mathrm{e}^{\frac{U(y)}{\theta}},\quad N=\frac{\theta}{\eta}\left(\int_0^L\mathrm{d}x\int_x^{x+L}\mathrm{d}y\,\mathrm{e}^{\frac{U(y)-U(x)}{\theta}}\right)^{-1} \tag{3}$$

where N is the normalization constant chosen so that $\int_0^L\mathrm{d}x\,P^{\rm st}(x)=1$. The steady state has a non-zero probability current $J^{\rm st}(x)$ given by

$$J^{\rm st}\equiv-\frac{1}{\eta}\left(U'(x)+\theta\frac{\partial}{\partial x}\right)P^{\rm st}(x)=N\left(1-\mathrm{e}^{-\frac{2\pi W}{\theta}}\right) \tag{4}$$

In this article, we study the low-temperature relaxation dynamics towards the steady state in the presence of a tilted periodic potential by the eigenfunction expansion method. Our main interest lies in the tilting dependence of the decay rate. As shown by van Kampen [8] the decay rate gives the Kramers rate if the metastable Landau potential is symmetric, and in this sense our aim is an extension of the Kramers theory to the decay to NESS. This paper is organized as follows. In Section 2, we present the framework of our analysis and relevant numerical data for eigenvalues of the FP operator. Section 3 treats the important theme on the boundary condition for eigenstates of the associated Schrödinger equation. In Section 3.1, the small tilting case is investigated with the real-valued WKB analysis. In Section 3.2, the large tilting case is treated, where we shall apply the complex-valued WKB method to the Schrödinger equation with the absorbing boundary condition deduced from PBC for the original FP equation. In Section 4, the slow decay due to the resonance tunneling is reported based on the numerical calculations. In the vicinity of the resonance, the analytic form of the decay rate is explored. Section 5 is devoted to the summary. In the Appendix, we show the details of the perturbative calculations of Section 3.2.

2. Eigenvalues of the Fokker–Planck operator

The WKB treatment of the FP equation has a long history since the monumental work by van Kampen [8]. Most of the studies, however, were limited to the system with a well-defined thermal equilibrium state [9,10,13,14]. This fact guaranteed a real-valued nature of the eigenvalues for the non-Hermitian FP operator, and one can reduce the FP equation to the eigenvalue problem of the associated Schrödinger operator (SO) with the same natural boundary condition as the probability density of the FP equation. On the other hand, relaxation dynamics towards the nonequilibrium steady state with the non-vanishing constant current demands a qualitatively different WKB approach. In fact the FP operator in such a system has complex eigenvalues in general.

This situation is recognized in our system with a tilted sinusoidal potential [15]

$$U(x)=U_0\cos\left(\frac{2\pi x}{L}\right)-\frac{2\pi W}{L}x \tag{5}$$

Putting eigenvalues of the non-Hermitian FP operator as $-E$ and substituting $P(x,t)=\mathrm{e}^{-Et}P(x)$ into Eq. (2), we have the eigenvalue problem,

$$-EP(x)=\frac{1}{\eta}\frac{\partial}{\partial x}\left(\frac{\partial U(x)}{\partial x}+\theta\frac{\partial}{\partial x}\right)P(x) \tag{6}$$

While the steady state in Eq. (3) is periodic, $P^{\rm st}(x+L)=P^{\rm st}(x)$, and is characterized by the zero Bloch wavenumber $k=0$, it is difficult to analyze the relaxation dynamics in general. Any initial distribution $P(x,0)$ which include $k\neq0$ Fourier components can relax towards $P^{\rm st}(x)$: the $k\neq0$ components will decay out in the course of time evolution. In the present work, however, we confine ourselves to the manifold of $k=0$, which makes the analysis of the decay phenomenon accessible. This implies that the time-dependent solution of the FP equation in Eq. (2) relaxing towards the steady state should satisfy the spatial PBC, $P(x+L,t)=P(x,t)$ and be constructed from solutions with a natural boundary condition $Q(x,t)$ ($\lim_{x\to\pm\infty}Q(x,t)=0$) as

$$P(x,t)=\sum_{n=-\infty}^{\infty}Q(x+nL,t) \tag{7}$$

Since the FP operator in Eq. (2) is invariant against spatial translation by L, it has Bloch-type eigenstates $\{P_{n,k}(x)\}$ and complex eigenvalues $\{E_{n,k}\}$. Noting the normalization matrix $\int_0^L \mathrm{d}x\, P^*_{k,n}(x)P_{k',n'}(x) = \delta_{k,k'}N^{(k)}_{n,n'}$ due to the non-Hermitian nature of the FP operator, the solution $P(x,t)$ in Eq. (7) is now written explicitly as

$$P(x,t) = \sum_n C_{n,k=0}P_{n,k=0}(x)\mathrm{e}^{-E_{n,k=0}t} \tag{8}$$

$$C_{n,k=0} = \sum_{n'} \left(N^{(0)}\right)^{-1}_{n,n'} \int_0^L \mathrm{d}x\, P^*_{n',k=0}(x)P(x,0), \quad C_{n,k\neq 0} = 0, \tag{9}$$

which starts from an arbitrary $k=0$ distribution $P(x,0)$ at $t=0$ and relaxes towards $P^{\mathrm{st}}(x)$.

In the manifold with $k=0$, the probability distribution can be expanded as $P(x) = \sum_n c_n \mathrm{e}^{\frac{2\pi \mathrm{i}x}{L}n}$. Then the eigenvalue problem (6) is reduced to

$$\left(\frac{2\pi}{L}\right)^2 \sum_m A_{n,m}c_m = \eta E c_n$$
$$A_{n,m} = -\left(\mathrm{i}nW + \theta n^2\right)\delta_{n,m} - \frac{nU_0}{2}\delta_{n-1,m} + \frac{nU_0}{2}\delta_{n+1,m} \tag{10}$$

which can be solved numerically by truncating the infinite dimensional matrix A to a large but finite dimensional matrix.

The zero-eigenvalue $E=0$ corresponds to the steady state. Under PBC, as is obvious from Eq. (8), the probability distribution approaches exponentially to the unique steady state, and the decay rate λ is obtained as the real part of the second smallest eigenvalue. Among many complex eigenvalues of Eq. (10), therefore, we have focused on the one with the second-smallest real part and its variation against various parameter values U_0, W (see Fig. 1). From Fig. 1 one can see that the eigenvalues with large positive real parts have nearly zero imaginary part. (See tails of solid lines in Fig. 1.) These eigenvalues correspond to the small tilting case. In fact, a pair of solid lines rapidly merge to the real axis as W decreases below U_0, ensuring the real-valued nature of eigenvalues in the case of small tilting.

U_0 and W dependence of the decay rate λ is shown in Fig. 2, which we have confirmed by numerically solving the FP equation in Eq. (2). There is a smooth but steep decrease of the decay rate around the crossover line of $U_0 \simeq W$, where the original potential minima disappear.

Later, the Schrödinger equation associated with the FP equation will be solved with use of the WKB method. In Fig. 3, the decay rates obtained by the WKB analysis are compared with the numerical eigenvalues of the FP operator.

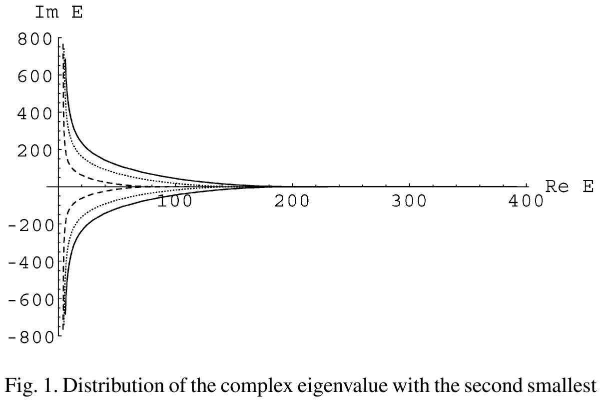

Fig. 1. Distribution of the complex eigenvalue with the second smallest real part for $0 \leqslant W \leqslant 20$ and fixed potential barriers $U_0 = 3$ (broken line), $U_0 = 7$ (broken-dotted line) and $U_0 = 10$ (solid line). The three lines rapidly merge to the real axis as W decreases below U_0.

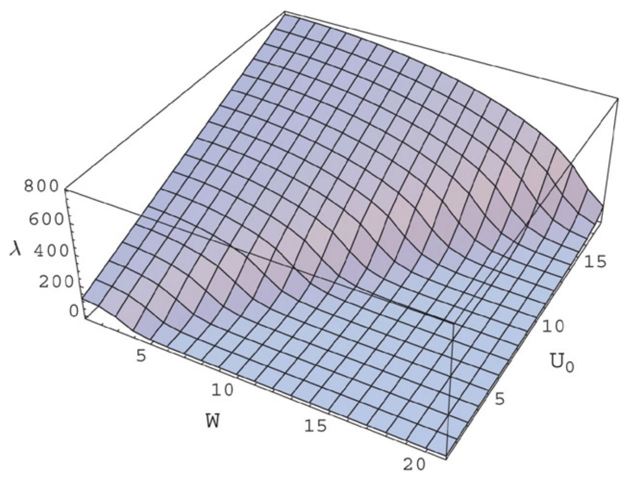

Fig. 2. W and U_0 dependence of the decay rate λ.

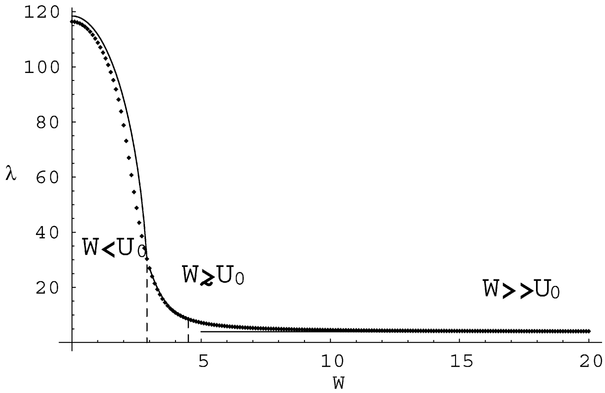

Fig. 3. W dependence of the decay rate λ for $U_0 = 3, \theta = 0.1$. Dots show the decay rates obtained from numerical diagonalization of the FP operator. Three solid lines are theoretical results (For small tilting case $W < U_0$ the decay rate λ is obtained by (35) as the first excited level $\hbar\omega_a$ of the associated Schrödinger equation (left part). For crossover regime $W \sim U_0$, λ is given as the numerical solution of (38) (middle part). For large tilting case $W \gg U_0$, the perturbative solution of (39) gives λ (right part).)

In the small tilting case, we impose PBC for the wavefunction of the Schrödinger equation and apply the Bloch theorem. The decay rate for $W < U_0$ is shown to be

$$\left(\frac{2\pi}{L}\right)^2 \sqrt{1 - \left(\frac{W}{U_0}\right)^2} \frac{U_0}{\eta}$$

In the large tilting case, we have recourse to the absorbing boundary condition and apply the WKB method which admits complex energies. The decay rate for $W \gg U_0$ is found to be $(2\pi/L)^2 \frac{\theta}{\eta}$ (with no W and U_0 dependence). The crossover region where W is comparable to U_0 is numerically analyzed based on this approach.

3. WKB analysis of probability distribution

The FP equation is transformed into the Schrödinger equation by the separation ansatz [8]

$$P(x,t) = \mathrm{e}^{-\frac{U(x)}{2\theta}} \phi(x) \mathrm{e}^{-Et} \tag{11}$$

Then one has

$$\theta \frac{\mathrm{d}^2}{\mathrm{d}x^2}\phi(x) + \big(E - V(x)\big)\phi(x) = 0 \tag{12}$$

where we redefined the eigenvalue as $E\eta \to E$, and defined the effective potential

$$V(x) \equiv \theta \left\{ \left(\frac{U'(x)}{2\theta} \right)^2 - \frac{U''(x)}{2\theta} \right\} \tag{13}$$

The Schrödinger operator (SO) in Eq. (12) looks Hermitian. Noting in Eq. (11) $U(x+L) = U(x) - 2\pi W$ and $P_{n,k}(x+L) = \mathrm{e}^{\mathrm{i}kL} P_{n,k}(x)$, however, the wave function $\phi(x)$ of the Schrödinger equation should satisfy the absorbing boundary condition,

$$\phi(x+L) = \mathrm{e}^{\mathrm{i}kL - \frac{2\pi W}{2\theta}} \phi(x) \tag{14}$$

which eventually breaks the Hermitian nature of SO.

In the small tilting case, the numerical evidence in the previous section has shown the real-valued nature of the second-lowest eigenvalue, indicating the recovery of Hermitian nature of SO. Therefore we reduce Eq. (14) to

$$\phi(x+L) = \mathrm{e}^{\mathrm{i}kL} \phi(x) \tag{15}$$

by assuming the absorbing term $\frac{2\pi W}{2\theta}$ being vanishing. The validity of this assumption will be verified by comparing between the analytic and numerical decay rates. Below we shall confine to the $k = 0$ manifold.

3.1. Small tilting case

Substituting the tilted sinusoidal potential (5) into (13), one has the effective potential,

$$V(x)=\frac{\pi^2}{L^2\theta}\left(U_0\sin\frac{2\pi x}{L}+W\right)^2+\frac{1}{2}\left(\frac{2\pi}{L}\right)^2U_0\cos\frac{2\pi}{L}x. \tag{16}$$

Since the first term is much larger than the second one in the low temperature regime $\theta \ll U_0$, the second one is omitted hereafter.

In solving Eq. (12) the low temperature condition allows us to use the WKB approximation, since θ corresponds to $\frac{\hbar^2}{2m}$ in the standard Schrödinger equation. In the case that the external force is weak ($W < U_0$), the effective potential $V(x)$ has three wells. We consider the energy levels for the eigenstates which experience all the three wells [18] (see Fig. 4).

In terms of the tilted potential $U(x)$, the weakness of the external force guarantees the existence of potential minima in Fig. 5. Let us denote the wave functions in each region $a,\dots,e$ bordered by classical turning points $x_0,\dots,x_5$ as $\phi_a,\dots,\phi_e$ and introduce the action integrals

$$S_a=\frac{1}{\hbar}\int_{x_0}^{x_1}p\,\mathrm{d}x,\quad M_b=\frac{1}{\hbar}\int_{x_1}^{x_2}p\,\mathrm{d}x,\quad S_c=\frac{1}{\hbar}\int_{x_2}^{x_3}p\,\mathrm{d}x,\quad M_d=\frac{1}{\hbar}\int_{x_3}^{x_4}p\,\mathrm{d}x \tag{17}$$

where the effective Planck constant $\hbar=\sqrt{2m\theta}$ with the effective mass m and $p=\sqrt{2m|E-V(x)|}$ (p stands for the momentum in a potential-well region). S and M are defined in each well and barrier, respectively. Neighboring localized wave functions are mutually related by the connection formula

$$\frac{1}{\sqrt{p}}\mathrm{e}^{\pm\mathrm{i}(S+\frac{\pi}{4})}\quad\big(E>V(x)\big)\quad\longleftrightarrow\quad\frac{1}{\sqrt{p}}\left(\mathrm{e}^{S}\pm\frac{\mathrm{i}}{2}\mathrm{e}^{-S}\right)\quad\big(E<V(x)\big) \tag{18}$$

where

$$S=\left|\frac{1}{\hbar}\int_{x}^{y_0}p\,\mathrm{d}x\right| \tag{19}$$

with y_0 being the classical turning point.

For example, ϕ_a and ϕ_b are related as

$$\phi_a(x)=\frac{1}{\sqrt{p}}\left(c_1\mathrm{e}^{-\frac{\mathrm{i}}{\hbar}\int_{x_0}^{x}p\,\mathrm{d}x}+c_2\mathrm{e}^{\frac{\mathrm{i}}{\hbar}\int_{x_0}^{x}p\,\mathrm{d}x}\right) \tag{20}$$

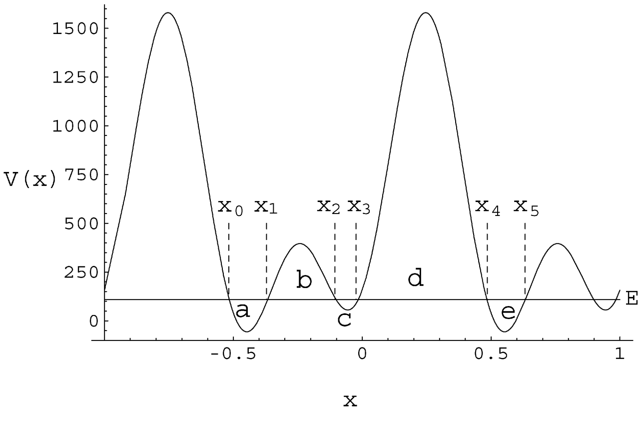

Fig. 4. Effective potential $V(x)$ and the real part of the eigenvalue of the FP operator with the second smallest real part E with the corresponding classical turning points $x_0,\dots,x_5$ for $W=1$, $U_0=3$.

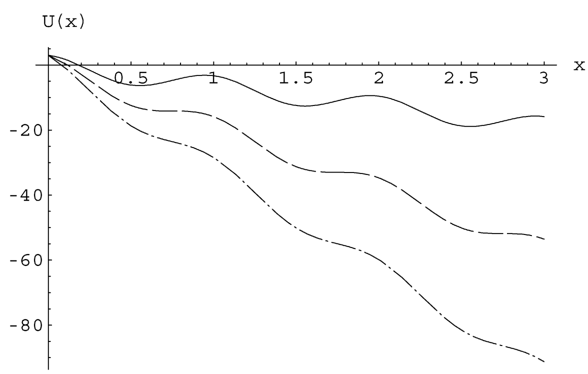

Fig. 5. Original tilted potential $U(x)$ in real space. Small tilting case (solid line), crossover region (broken line), and large tilting case (broken-dotted line).

$$\phi_b(x)=\frac{1}{\sqrt{|p|}}\left\{c_1\mathrm{e}^{-\mathrm{i}S_a}\left(\mathrm{e}^{\frac{1}{\hbar}\int_{x_1}^{x}p\,\mathrm{d}x}+\frac{\mathrm{i}}{2}\mathrm{e}^{-\frac{1}{\hbar}\int_{x_1}^{x}p\,\mathrm{d}x}\right)+c_2\mathrm{e}^{\mathrm{i}S_a}\left(\mathrm{e}^{\frac{1}{\hbar}\int_{x_1}^{x}p\,\mathrm{d}x}-\frac{\mathrm{i}}{2}\mathrm{e}^{-\frac{1}{\hbar}\int_{x_1}^{x}p\,\mathrm{d}x}\right)\right\} \tag{21}$$

In the same way, one obtains the expression for $\phi_e(x)$ as

$$\phi_e(x)=\frac{1}{\sqrt{p}}\left\{(Ac_1+Bc_2)\mathrm{e}^{-\frac{\mathrm{i}}{\hbar}\int_{x_4}^{x}p\,\mathrm{d}x}+(Cc_1+Dc_2)\mathrm{e}^{\frac{\mathrm{i}}{\hbar}\int_{x_4}^{x}p\,\mathrm{d}x}\right\} \tag{22}$$

where A, B, C and D are given as

$$\begin{aligned}
A&=\mathrm{e}^{\mathrm{i}S_a}\left\{\frac{1}{2}\left(\mathrm{i}\mathrm{e}^{M_b}\sin S_c+\frac{1}{4}\mathrm{e}^{-M_b}\cos S_c\right)\mathrm{e}^{-M_d}+2\left(\mathrm{e}^{M_b}\cos S_c+\frac{\mathrm{i}}{4}\mathrm{e}^{-M_b}\sin S_c\right)\mathrm{e}^{M_d}\right\}\\
B&=\mathrm{e}^{-\mathrm{i}S_a}\left\{\frac{1}{2}\left(\mathrm{e}^{M_b}\sin S_c+\frac{\mathrm{i}}{4}\mathrm{e}^{-M_b}\cos S_c\right)\mathrm{e}^{-M_d}-2\left(\mathrm{i}\mathrm{e}^{M_b}\cos S_c+\frac{1}{4}\mathrm{e}^{-M_b}\sin S_c\right)\mathrm{e}^{M_d}\right\}\\
C&=\mathrm{e}^{\mathrm{i}S_a}\left\{\frac{1}{2}\left(\mathrm{e}^{M_b}\sin S_c-\frac{\mathrm{i}}{4}\mathrm{e}^{-M_b}\cos S_c\right)\mathrm{e}^{-M_d}-2\left(-\mathrm{i}\mathrm{e}^{M_b}\cos S_c+\frac{1}{4}\mathrm{e}^{-M_b}\sin S_c\right)\mathrm{e}^{M_d}\right\}\\
D&=\mathrm{e}^{-\mathrm{i}S_a}\left\{\frac{1}{2}\left(-\mathrm{i}\mathrm{e}^{M_b}\sin S_c+\frac{1}{4}\mathrm{e}^{-M_b}\cos S_c\right)\mathrm{e}^{-M_d}+2\left(\mathrm{e}^{M_b}\cos S_c-\frac{\mathrm{i}}{4}\mathrm{e}^{-M_b}\sin S_c\right)\mathrm{e}^{M_d}\right\}
\end{aligned} \tag{23}$$

On the other hand, with use of the Bloch theorem in Eq. (15) based on the periodicity of the effective potential V, ϕ_e and ϕ_a should be related as

$$\phi_e(x+L)=\mathrm{e}^{\mathrm{i}kL}\phi_a(x) \tag{24}$$

where k is the wave number. This relation gives a constraint to guarantee the nontrivial coefficients (c_1,c_2) of ϕ_a and ϕ_e:

$$\begin{vmatrix} A-\mathrm{e}^{\mathrm{i}kL} & B\\ C & D-\mathrm{e}^{\mathrm{i}kL}\end{vmatrix}=0 \tag{25}$$

which can be rewritten as

$$\mathrm{e}^{\mathrm{i}kL}=\cos(kL)+\mathrm{i}\sin(kL)=\frac{1}{2}(A+D)\pm\mathrm{i}\sqrt{1-\frac{1}{4}(A+D)^2} \tag{26}$$

Here we have used the fact $AD-BC=1$. At low temperatures the tunneling integrals are sufficiently large, $M_b\gg 1$ and $M_d\gg 1$. Then we can make an approximation:

$$\frac{1}{4}(A+D)^2\cong 4\mathrm{e}^{2M_b}\mathrm{e}^{2M_d}\cos^2(S_a)\cos^2(S_c) \tag{27}$$

Since (27) should satisfy (26), $|\cos S_a|$ and $|\cos S_c|$ must be sufficiently small and can be approximated as

$$\begin{aligned}
&\cos(S_{a,c})\simeq(-1)^{n_{a,c}}\left\{S_{a,c}-\pi\left(n_{a,c}+\frac{1}{2}\right)\right\}\\
&\sin(S_{a,c})\simeq(-1)^{n_{a,c}}
\end{aligned} \tag{28}$$

Furthermore, using the harmonic approximation in the neighborhood of the local minima $x_{\min}^{a,c}$, the actions can be evaluated as

$$S_{a,c}=\frac{\pi}{\hbar\omega_{a,c}}(E-V_{0a,c}) \tag{29}$$

where $\omega_{a,c}=\sqrt{\frac{2\theta}{\hbar^2}V''(x_{\min}^{a,c})}$ is the curvature of the local minima, and $V_{0a,c}$ stands for the local minima of $V(x)$. Then Eq. (26) gives the quantization condition for eigenvalues E

$$\begin{aligned}
\cos(kL)&=\frac{1}{2}(A+D)\\
&=\frac{1}{2}\left\{\left(4\mathrm{e}^{M_b+M_d}+\frac{1}{4}\mathrm{e}^{-M_b-M_d}\right)\cos(S_a)\cos(S_c)-\left(\mathrm{e}^{-M_b+M_d}+\mathrm{e}^{M_b-M_d}\right)\sin(S_a)\sin(S_c)\right\}
\end{aligned}$$

$$\simeq \frac{1}{2}\Bigg\{\left(4e^{M_b+M_d}+\frac{1}{4}e^{-M_b-M_d}\right)\left(\left(n_a+\frac{1}{2}\right)\pi-\frac{\pi}{\hbar\omega_a}(E-V_{0a})\right)\left(\left(n_c+\frac{1}{2}\right)\pi-\frac{\pi}{\hbar\omega_c}(E-V_{0c})\right) - \left(e^{M_b-M_d}+e^{-M_b+M_d}\right)\Bigg\}(-1)^{n_a+n_c} \tag{30}$$

Solving the quadratic equation of E in (30), we obtain the lowest few eigenvalues within the $k=0$ manifold,

$$E_\pm = E_{0+} \pm \sqrt{E_{0-}^2+\epsilon} \tag{31}$$

$$\simeq E_{0+} \pm \left(E_{0-}+\frac{\epsilon}{2E_{0-}}\right) \tag{32}$$

where $E_{0\pm}$ stand for the harmonic oscillator levels at the wells and ϵ is a correction due to tunneling, which are defined as

$$E_{0\pm} = \frac{1}{2}\left\{V_{0a} \pm V_{0c} + \hbar\omega_a\left(n_a+\frac{1}{2}\right) \pm \hbar\omega_c\left(n_c+\frac{1}{2}\right)\right\}$$

$$\epsilon \equiv \epsilon(k=0) = \frac{\hbar^2\omega_a\omega_c}{\pi^2}\frac{e^{-2M_b}+e^{-2M_d}+2(-1)^{n_a+n_c}e^{-M_b-M_d}\cos k}{4+\frac{1}{4}e^{-2M_b-2M_d}} \tag{33}$$

where we have assumed that tunneling term ϵ is negligible compared with the difference between the vacuum energies of the two neighboring wells, E_{0-}, based on the numerical evidence. The opposite case, i.e. the tunneling term becomes dominant $\epsilon \gg E_{0-}$, is explored in the context of the resonance in the Section 4.

In general, the eigenvalues form subbands with their width given by the tunneling term ϵ, although we confine ourselves to the $k=0$ state in each of the subbands. At

$$x_{\min}^a = \frac{L}{2\pi}\left(n\pi - (-1)^n \arcsin\frac{W}{U_0}\right)$$

we find

$$V_{0a} = V(x_{\min}) \simeq -\frac{1}{2}\left(\frac{2\pi}{L}\right)^2\sqrt{1-\left(\frac{W}{U_0}\right)}U_0$$

and

$$\hbar\omega_a \simeq \left(\frac{2\pi}{L}\right)^2\sqrt{1-\left(\frac{W}{U_0}\right)^2}U_0 \tag{34}$$

Noting further that $V_{0a}+\frac{1}{2}\hbar\omega_a \simeq V_{0c}+\frac{1}{2}\hbar\omega_c \simeq 0$, one can confirm the lowest eigenvalue $E_- \simeq 0$, which is responsible to the steady state. Since the tunneling term is small compared to $\hbar\omega_a$, one finds the decay rate (the second-lowest eigenvalue),

$$\eta\lambda = E_+ \simeq \hbar\omega_a = \left(\frac{2\pi}{L}\right)^2\sqrt{1-\left(\frac{W}{U_0}\right)^2}U_0 \tag{35}$$

We have confirmed numerically that this expression gives a good approximation for the decay rate in the small tilting case (see Fig. 3).

Now we can explain the external force W dependence of the decay rate. From (35) one has the monotonic W dependence of the decay rate. Intuitively, this behavior of the decay rate is explained in terms of tunneling process as follows. The energy level $\hbar\omega_a = \sqrt{2\theta V''(x_{\min}^a)}$ is a monotonic function of the curvature of the potential minimum $V''(x_{\min}^a)$ which decreases for increasing W, because the potential barrier becomes lower and finally the barrier disappears as W increases.

3.2. Large tilting case

The separation ansatz

$$P(x,t) = \mathrm{e}^{-\frac{U(x)}{2\theta}} \phi(x) \mathrm{e}^{-Et}$$

in Eq. (11) seems to contain a divergent term coming from $\mathrm{e}^{\frac{2\pi Wx}{2L\theta}}$ involved in $\mathrm{e}^{-\frac{U(x)}{2\theta}}$. This problem was overcome by choosing the absorbing boundary condition in Eq. (14). Confining ourselves to $k=0$ states as in the previous subsection, we have

$$\phi(x+L) = \mathrm{e}^{-\frac{2\pi W}{2\theta}} \phi(x) \tag{36}$$

With use of the complex-valued WKB method, Eq. (36) leads to the quantization condition for the complex eigenvalues $E = E_1 + \mathrm{i}E_2$ as

$$\mathrm{e}^{\pm \mathrm{i} \int_0^L \mathrm{d}x \sqrt{\theta^{-1}(E_1 - V(x) + \mathrm{i}E_2)}} = \mathrm{e}^{-\frac{2\pi W}{2\theta} + 2n\pi \mathrm{i}} \tag{37}$$

with $V(x)$ given in Eq. (16).

Remarkably there is no classical turning point on the real axis, and the energy becomes complex, as is confirmed numerically for the strongly tilted case (see Fig. 1). Then the decay rate λ is given by the real part of the eigenvalue with the second smallest part E_1. The existence of the imaginary part E_2 implies that the asymptotic behavior is oscillating.

Noting again that the second term of (16) is suppressed at low temperatures, the WKB quantization condition (37) is rewritten as

$$\frac{\pi W}{\theta L} \int_0^L \sqrt{1 + 2\frac{U_0}{W} \sin\frac{2\pi x}{L} + \left(\frac{U_0}{W}\right)^2 \sin^2\frac{2\pi x}{L} - \frac{\theta L^2}{\pi^2 W^2}(E_1 + \mathrm{i}E_2)} = -\frac{\pi W}{\theta} + \mathrm{i}2\pi n \tag{38}$$

For the large tilting case $W \gg U_0$, we can solve this equation perturbatively with the expansion parameter U_0/W (see Appendix A). Since it is numerically shown that the integer n is ± 1 for the parameter range $3 \leqslant U_0 \leqslant 20$, $U_0 \leqslant W \leqslant 20$, we investigate the case that $n = \pm 1$. As a result, we obtain for large W

$$E_1 = \left(\frac{2\pi}{L}\right)^2 \frac{\theta}{\eta}, \qquad E_2 = \pm\left(\frac{2\pi}{L}\right)^2 \frac{W}{\eta} \tag{39}$$

These results well agree with those from the numerical diagonalization of the FP operator. It is interesting that for large W, the decay rate E_1 saturates and depends only on the temperature, the period and the damping coefficient. It is also worth noting that E_2, which represents the oscillation frequency in the asymptotic behavior, is proportional to W and does not depend on U_0.

4. Resonance tunneling and slow decay

In this section, we investigate the more general case where the original potential includes a higher Fourier component,

$$U(x) = U_0\left(\cos\frac{2\pi x}{L} + \alpha \sin\frac{4\pi x}{L}\right) - \frac{2\pi W}{L}x \tag{40}$$

In the same way as Eq. (10), one has the eigenvalue problem of the FP operator

$$\left(\frac{2\pi}{L}\right)^2 \sum_m A_{n,m} c_m = \eta E c_n$$

$$A_{n,m} = -(\mathrm{i}nW + \theta n^2)\delta_{n,m} - \frac{nU_0}{2}\delta_{n-1,m} + \frac{nU_0}{2}\delta_{n+1,m} + \mathrm{i}U_0\alpha n\delta_{n,m+2} + \mathrm{i}U_0\alpha n\delta_{n,m-2} \tag{41}$$

The numerical decay rate shows non-monotonic dependence on the tilting (see Fig. 7). In terms of the original potential $U(x)$, the anomalously-slow relaxation; (a sudden drop of λ around $W = 1.7$ in Fig. 7) can be attributed to as the appearance of an extra barrier within a period.

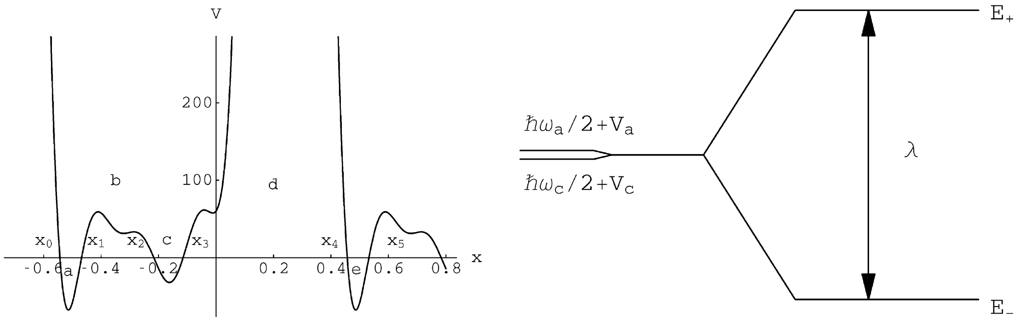

(a) (b)

Fig. 6. (a) Effective periodic potential $V(x)$ and regions a, …, e bordered by the classical turning points $x_0, \ldots, x_5$ in the parameter range $U_0 = 3, W = 1.7, \theta = 0.1, \alpha = 0.3$ where slow decay is observed. (b) Degenerated energy levels split due to the tunneling, which gives the decay rate λ.

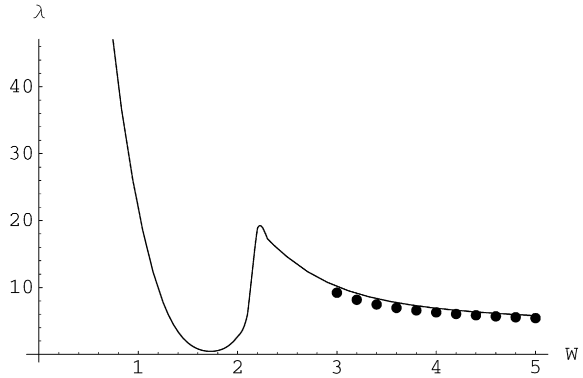

Fig. 7. W dependence of the decay rate λ in the existence of a higher Fourier component for $U_0 = 3, \theta = 0.1, \alpha = 0.3$. The solid line show the decay rate obtained from numerical diagonalization of the FP operator. Dots are the decay rate obtained by the WKB formula with absorbing boundary condition for $W > U_0$. Slow decay rate is seen around $W = 1.7$.

As in the previous section, we analytically explore the decay rate with the aid of the real and the complex valued WKB analyses.

The corresponding effective potential takes a form as in Fig. 6(a). One finds that the barrier d is extremely high, and the low-lying states in the structured wells between those barriers contribute to the decay rate, which is given by the tunneling between the degenerate levels of the wells a and c as in Fig. 6(a). We assume that the classical turning points are on the real-axis, since the decay process includes the escape over the barrier d, the decay rate and thus the first excited level is much smaller than the typical barrier height. Around the tiling W accompanied with the slow relaxation, the tilting W is small compared to the barrier height U_0, the decay rate might be calculated with use of WKB approximation under PBC for the associated Schrödinger equation. As in the Subsection 3.1, we should connect the localized wave functions and apply the Bloch theorem (32).

In the vicinity of the slow relaxation, due to the tunneling effect the degenerated energies split as in the Fig. 6(b) [8,10] and the decay rate λ is given as the difference of the lowest two energies, which is expressed by the tunneling integral, i.e., in terms of $E_\pm$ and ϵ defined by Eq. (31)

$$\lambda = E_+ - E_- = 2\sqrt{\epsilon + E_{0-}^2} \simeq \sqrt{\frac{\hbar^2 \omega_a \omega_c}{\pi^2}} \mathrm{e}^{-M_b} \left(1 + \frac{E_{0-}^2}{2}\right) \tag{42}$$

with

$$E_{0-} = \frac{1}{2}\left(\left(V_{0a} + \frac{\hbar\omega_a}{2}\right) - \left(V_{0c} + \frac{\hbar\omega_c}{2}\right)\right)$$

where we used the fact $M_b \ll M_d$ and neglected the terms proportional to e^{-M_d} (see Fig. 6(a)). Since the original potential has single maximum at a point $x = y$ in the barrier region, $[x_1, x_2]$, the tunneling integral M_b is perturbatively calculated as [13]

$$\begin{aligned}\theta M_b &= \int_{x_1}^{x_2} \sqrt{\frac{U'^2}{4} - \frac{\theta U''}{2}}\,\mathrm{d}x \\ &= \int_{x_1}^{y-\Delta} \frac{U'}{2}\left(1 - \frac{\theta U''}{U'^2}\right)\mathrm{d}x + \int_{y-\Delta}^{y+\Delta} \sqrt{\frac{\theta|U''|}{2}}\sqrt{1 - \frac{U'^2}{2\theta U''}}\,\mathrm{d}x - \int_{y+\Delta}^{x_2} \frac{U'}{2}\left(1 - \frac{\theta U''}{U'^2}\right)\mathrm{d}x \\ &= \frac{2U(y) - U(x_1) - U(x_2)}{2} - \theta\bigl(1 - \sqrt{2} - \operatorname{arcsinh}(1)\bigr) + \theta \log\sqrt{\frac{U'(x_1)|U'(x_2)|}{2\theta|U''(y)|}}\end{aligned} \tag{43}$$

with $\Delta = \sqrt{\frac{2\theta}{|U''(y)|}}$. Thus the decay rate can be rewritten in the form of the Kramers rate,

$$\lambda = \frac{1}{\pi}\mathrm{e}^{2-\sqrt{2}-\operatorname{arcsinh}(1)}\sqrt{\sqrt{U''(x^a_{\min})U''(x^c_{\min})}\,\bigl|U''(y)\bigr|}\left(1 + \frac{E_{0-}^2}{2}\right)\mathrm{e}^{-\frac{\Delta U_1 + \Delta U_2}{2\theta}} \tag{44}$$

with $\Delta U_1 = U(y) - U(x^a_{\min})$, $\Delta U_2 = U(y) - U(x^c_{\min})$. It is remarkable that the activation energy is now given by the arithmetic mean of two partial barrier heights [13].

5. Summary

The low-temperature ($\theta = k_B T$) decay of the thermal diffusion in the tilted periodic potential described by the Fokker–Planck (FP) equation, is investigated in terms of the (generalized) WKB method. The nonequilibrium steady state demands a subtle approach to the asymptotic decay phenomenon, qualitatively different from the one often used in the context of the decay to the thermal equilibrium. However, we have confined ourselves to the manifold of $k = 0$ which includes the steady state. This recourse makes the analysis of the decay phenomenon accessible.

While eigenvalues of the FP operator are complex in general, in a small tilting case ($W < U_0$) the imaginary parts of the eigenvalues are shown to be vanishing. Then the Schrödinger equation associated with FP equation has the WKB solution satisfying PBC. Among the continuum of Bloch states, the zero-wavenumber eigenvalues are essential. The lowest eigenvalue is responsible for the steady state and the decay rate is determined by the second-lowest eigenvalue within the zero-wavenumber manifold. The parameter dependence of the decay rate is explained by the tunneling process through a triple-well effective periodic potential. The decay rate λ is given by

$$\left(\frac{2\pi}{L}\right)^2\sqrt{1 - \left(\frac{W}{U_0}\right)^2}\frac{U_0}{\eta}$$

In the large tilting case ($W \gg U_0$), the imaginary parts of the eigenvalues of the FP operator are crucial and conservative approach collapses. We apply the complex-valued WKB method to the Schrödinger equation with the absorbing boundary condition, finding the decay phenomenon characterized by the decay rate $E_1 = (\frac{2\pi}{L})^2\frac{\theta}{\eta}$ and the oscillation frequency $E_2 = (\frac{2\pi}{L})^2\frac{W}{\eta}$. The intermediate tilting case is also explored, and our theoretical results from the WKB analysis explain W and U_0 dependence of the numerical decay rate quite well for all parameter ranges in Fig. 3. We also investigated the case that the original potential includes a higher Fourier component. Numerical eigenvalues becomes astonishingly small at some value of tilting, which can be attributed to the degeneracy of unperturbed energy levels. In the vicinity of the resonance, to remove the degeneracy we evaluate the tunneling integral perturbatively with respect to the temperature, and the decay rate turns out to resemble the so-called Kramers escape rate for metastable state. The decay phenomena starting from $k \neq 0$ distributions and the contribution from continuous spectra to nonexponential decays will constitute subjects which we intend to study in future.

Acknowledgements

T.M. thanks Prof. S. Tasaki for valuable comments including the advice about calculation in Eq. (37). This work is partly supported by a JSPS Research Fellowship for young scientists and 21st Century COE Program (Holistic research and Education, Culture, Sports, Science and Technology). A.S. and K.N. are grateful to JSPS for the financial support to the Fundamental Research.

Appendix A. Perturbative analysis of the complex eigenvalue problem for large tilting case

For the large tilting case ($W \gg U_0$), the WKB quantization condition under the absorbing boundary condition is given by Eq. (37) or equivalently by

$$\mathrm{i}\int_0^L \mathrm{d}x\sqrt{\theta^{-1}(E_1 - V(x) + \mathrm{i}E_2)} = -\frac{\pi W}{\theta} + 2n\pi\mathrm{i} \tag{A.1}$$

We have solved Eq. (A.1) perturbatively with use of the expansion parameter $\epsilon = \frac{U_0}{W}$ as follows.

We restrict ourselves to the case $n = \pm 1$ which is observed numerically in the parameter range $3 \leqslant U_0 \leqslant 20$, $U_0 \leqslant W \leqslant 20$ and use a branch of square-root with positive imaginary part in the left-hand side of (A.1) (another branch does not satisfy (A.1)). At first, we note that (A.1) is equivalent to

$$-\int_0^L \mathrm{d}x\left(\sqrt{\frac{1}{2}\left(A + \sqrt{A^2 + B^2}\right)} + \mathrm{i}\sqrt{\frac{1}{2}\left(-A + \sqrt{A^2 + B^2}\right)}\right) = -L + \mathrm{i}\frac{2\theta L}{W}$$

$$A = \left(1 + \epsilon\sin\frac{2\pi x}{L}\right)^2 - \frac{\theta L^2}{\pi^2 W^2}E_1, \qquad B = \frac{\theta L^2}{\pi^2 W^2}E_2 \tag{A.2}$$

We expand eigenvalue $E_1 + \mathrm{i}E_2$ up to the second order of ϵ as

$$\frac{\theta L^2}{\pi^2 W^2}E_1 = A_1\epsilon + A_2\epsilon^2 + \mathrm{O}(\epsilon^3), \qquad \frac{\theta L^2}{\pi^2 W^2}E_2 = B_1\epsilon + B_2\epsilon^2 + \mathrm{O}(\epsilon^3) \tag{A.3}$$

Then the real part of Eq. (A.2) is expanded in ϵ as

$$\int_0^L \mathrm{d}x\left\{1 + \frac{1}{2}\left(-A_1 + 2\sin\frac{2\pi x}{L}\right)\epsilon + \left(\frac{-1}{8}\left(-A_1 + 2\sin\frac{2\pi x}{L}\right)^2 - \frac{1}{2}A_2 + \frac{1}{2}\sin^2\frac{2\pi x}{L} + \frac{1}{8}B_1^2\right)\epsilon^2 + \mathrm{O}(\epsilon^3)\right\} = L \tag{A.4}$$

Noting that coefficients of each power of ϵ should vanish and using

$$\int_0^L \mathrm{d}x\sin\frac{2\pi x}{L} = 0, \qquad \int_0^L \mathrm{d}x\sin^2\frac{2\pi x}{L} = \frac{1}{2}$$

we obtain

$$A_1 = 0, \qquad A_2 = \frac{1}{4}B_1^2 \tag{A.5}$$

In the same way, the imaginary part of (A.2) is (provided $A_1 = 0$)

$$\int_0^L \mathrm{d}x\left\{\frac{B_1}{2}\epsilon + \frac{1}{2}\left(B_2 - B_1\sin\frac{2\pi x}{L}\right)\epsilon^2 + \mathrm{O}(\epsilon^3)\right\} = \frac{2\theta L}{W} \tag{A.6}$$

Thus one has

$$A_2 = \frac{4\theta^2}{U_0^2}, \qquad B_1 = \pm\frac{4\theta}{U_0} \tag{A.7}$$

From these expressions the eigenvalue is given by Eq. (39). As shown in Fig. 3 this estimation of E_1 is very accurate for $W \gg U_0$.

References

[1] J.W.M. Frenken, J.F. Van der Veen, Phys. Rev. Lett. 54 (1985) 134;
B. Pluis, et al., Phys. Rev. Lett. 59 (1987) 2678;
T.R. Linderoth, S. Horch, E. Laegsgaard, I. Stensgaard, F. Besenbacher, Phys. Rev. Lett. 78 (1997) 4978;
P. Talkner, E. Hershkovitz, E. Pollak, P. Hänggi, Surf. Sci. 437 (1999) 198.

[2] A. Barone, G. Paterno, Physics and Applications of the Josephson Effect, Wiley, New York, 1982.

[3] A. Ajdari, J. Prost, Proc. Natl. Acad. Sci. U.S.A. 88 (1991) 4468;
G.I. Nixon, G.W. Slater, Phys. Rev. E 53 (1996) 4969.

[4] P. Hänggi, P. Talkner, M. Borkovec, Rev. Mod. Phys. 62 (1990) 251.

[5] P. Reimann, Phys. Rep. 361 (2002) 57.

[6] C.R. Doering, W. Horstemke, J. Riordan, Phys. Rev. Lett. 72 (1994) 2984.

[7] P. Reimann, C. Van den Broeck, H. Linke, P. Hänggi, J.M. Rubi, A. Pérez-Madrid, Phys. Rev. Lett. 87 (2001) 010602;
P. Reimann, C. Van den Broeck, H. Linke, P. Hänggi, J.M. Rubi, A. Pérez-Madrid, Phys. Rev. E 65 (2002) 031104.

[8] N.G. van Kampen, J. Stat. Phys. 17 (1977) 71;
N.G. van Kampen, Suppl. Prog. Theor. Phys. 64 (1978) 389;
N.G. van Kampen, Stochastic Processes in Physics and Chemistry, second ed., North-Holland, Amsterdam, 1981.

[9] B. Caroli, C. Caroli, B. Roulet, J. Stat. Phys. 21 (1979) 415;
B. Caroli, C. Caroli, B. Roulet, J. Stat. Phys. 26 (1981) 83;
H. Tomita, A. Ito, H. Kidachi, Prog. Theor. Phys. 56 (1976) 786.

[10] K. Nakamura, T. Sasada, Phys. Lett. A 74 (1979) 379.

[11] O. Galkin, P.G. Vekilov, J. Crystal Growth 232 (2001) 63.

[12] G. Nicolis, C. Nicolis, Physica A 323 (2003) 139.

[13] T. Monnai, A. Sugita, K. Nakamura, Phys. Rev. E 74 (2006) 061116.

[14] E. Arvedson, M. Wilkinson, B. Mehlig, K. Nakamura, Phys. Rev. Lett. 96 (2006) 030601.

[15] P. Noziere, G. Iche, J. Physique 40 (1979) 225;
W. Dieterich, et al., Z. Phys. B 27 (1977) 177.

[16] J.L. Lebowitz, P.G. Bergmann, Ann. Phys. 1 (1957) 1.

[17] H. Risken, The Fokker Planck Equation, Springer-Verlag, Berlin, 1989.

[18] D. ter Haar, Selected Problems in Quantum Mechanics, Academic-Verlag, New York Press, 1964;
S. Ohta, K. Nakamura, J. Phys. C 14 (1981) L427.